The current issue and full text archive of this journal is available at
www.emeraldinsight.com/0961-5539.htm

Buoyancy-driven flow of a viscous incompressible fluid in an open-ended rectangular cavity with permeable horizontal surfaces

M.A. Hossain and S. Asghar
Department of Mathematics, COMSATS Institute of Information Technology, Islamabad, Pakistan, and
Rama Subba Reddy Gorla
Department of Mechanical Engineering, Cleveland State University, Cleveland, Ohio, USA

Received 25 November 2008
Reviewed 16 June 2009
Revised 11 September 2009
Accepted 21 September 2009

Abstract

Purpose – The purpose of this paper is to consider the unsteady natural convection flow of a viscous incompressible fluid, which is induced by differential heating on the solid vertical boundary of an open-ended rectangular cavity with the two horizontal surfaces which are permeable and maintained at the temperature of ambient fluid. Attention is focused on how the flow and heat transfer is affected by variations of the buoyancy force, as well as by the permeability of the surfaces.

Design/methodology/approach – An upwind finite-difference method in conjunction with a successive over-relaxation iteration technique is used to solve the governing boundary layer equations. To do this, the first and second derivatives were approximated by central differences and were used in the vorticity, energy and Poisson equations. To preserve the conservative property, the finite-difference forms of the vorticity and energy equations were written in conservative form for the convective terms.

Findings – Local rate of heat transfer from the heated surface increases owing to an increase in the value of *Ra*. In the region near the bottom surface, the heat transfer from the left vertical surface decreases, but that increases in the region near the upper surface. Due to blowing of fluid through the permeable surfaces, the rate of heat transfer is higher than the situation where fluid is being withdrawn. This difference was found to be higher in the case of larger value of *Ra*.

Research limitations/implications – The analysis is valid for unsteady, two-dimensional natural convection flow of a viscous fluid filled in an open-ended rectangular enclosure. An extension to three-dimensional flow case is left for future work.

Practical implications – The method is very useful to analyze solar receiver systems, fire research, electronic cooling, brake housing of an aircraft and many environmental geothermal processes.

Originality/value – The results of this study may be of some interest to engineers interested in heat transfer in ventilated rooms or enclosures.

Keywords Convection, Flow, Permeability, Surface properties of materials

Paper type Research paper

Nomenclature

C_p	specific heat at constant pressure (J/kg K)	Nu_a	average Nusselt number
g	gravitational acceleration (m/s)	P	fluid pressure (Pa)
H	enclosure height (m)	Pr	Prandtl number
L	enclosure breadth (m)	Ra	Rayleigh number
Nu	local Nusselt number	Re	Reynolds number
		t	time (s)

International Journal of Numerical Methods for Heat & Fluid Flow
Vol. 20 No. 7, 2010
pp. 759-772

0961-5539
DOI 10.1108/09615531011065557

T	temperature (°C)
S	bowing and withdrawal parameter
U, V	dimensionless velocity components in X- and Y-direction
V_0	transpiration velocity (m/s)
u, v	velocity in x- and y-direction (m/s)
x, y	Cartesian coordinates (L)
X, Y	dimensionless coordinates
β	coefficient of thermal expansion of fluid (K^{-1})
G	dimensionless temperature
μ	effective dynamic viscosity (Pa/s)
ν	effective kinematic viscosity (μ/ρ)
ρ	fluid density at reference temperature (T_c)
τ	dimensionless time
ψ	dimensionless stream function
Ω	dimensionless vorticity function

1. Introduction

In recent years, increasing attention has taken place among the researchers on the buoyancy-driven flows of viscous incompressible fluids in open-ended enclosures because of the various practical applications. Such applications include solar thermal receiver systems, fire research, cooling of electronic equipment and energy conservation in buildings. One should mention that the main characteristic of buoyancy-driven flows and heat transfer in open-ended cavities is its basic geometry, which reveals the interactions and the influence of the inner and outer regions of the cavity on the flow and temperature fields.

Penot (1982) conducted a numerical study of two-dimensional (2D) natural convection in an isothermal open square enclosure. The results of this study showed that the flow unsteadiness arises for large values of Grashof number and that the flow field approaching the open cavity depends on the far field boundary conditions. Other Problems involving natural convection in open enclosures were studied by Doria (1974) for predicting unsteady flows of multi-component gases with strong buoyancy effects and by Jacobs *et al.* (1974, 1976) in modeling circulation above city streets and geothermal reservoirs. Chen *et al.* (1985) and Serans and Kyriakides (1982) had also conducted experimental studies by modeling the solar systems. Chan and Tien (1982) performed a numerical steady-state study of laminar natural convection in a 2D square open cavity with a heated vertical wall and two insulated horizontal walls. The results of this study illustrated the effect of the open boundary on the basic flow patterns. Later on, the same authors (Chan and Tien, 1985) investigated numerically laminar steady-state natural convection in a 2D rectangular open cavity by imposing approximate boundary conditions at the open side of the enclosure. Vafai and Ettefagh (1990a, b) conducted a comprehensive study for investigating basic aspects and physics of the flow field within the open-ended structures and the effect of extended computational domain on flow and heat transfer inside the open-ended cavity and its immediate surroundings. Vafai and Ettefagh (1990a, b) established that the extent of the enlarged computational domain has a substantially larger effect than previously reported by other investigators. Following Chan and Tien (1985), investigation of natural convection flow in a square open cavity with one side heated and other two adiabatic as well as heated has been performed by Angirasa *et al.* (1996, 2002) by solving the vorticity transport and stream function formulation. In these problems, the computations were carried out without considering an outer region by specifying appropriate set of boundary conditions at the window for temperature as proposed by Chan and Tien (1985).

Recently, Bilgen and Oztop (2005), carried out a study on inclined partially open square cavity, which is formed by adiabatic walls and a partial opening and also assuming the surface of the wall inside the cavity facing the partial opening to be isothermal. On the other hand, investigation on natural convection heat transfer in partially open inclined square cavity with discrete heat source at the bottom surface was conducted by Müftüöglu and Bilgen (2008). In this investigation the authors determined optimum positions of discrete heat source by maximizing the conductance and then studied heat transfer and volume flow rate with discrete heat source at their optimum positions. Very recently, the problem posed by Angirasa *et al.* (1996, 2002) the natural convection in an open-ended cavity is simulated by Mohamad *et al.* (2009) using lattice Boltzmann method.

Here, also we are addressing an investigation on an unsteady natural convection flow of a viscous incompressible fluid enclosed in an open-ended rectangular cavity, posed by Angirasa *et al.* (1996, 2002). The vertical side opposite to the open end is maintained at a uniform temperature which is higher than that of the ambient temperature. We further have considered that the horizontal surfaces are permeable and maintained at the temperature of the ambient fluid. So far the authors' concern, this problem has not been discussed in the literature. With this understanding, the resulting dimensionless equations are simulated numerically using an upwind difference scheme together with successive over-relaxation method. Results are obtained for different values of the Rayleigh number, *Ra*, and Reynolds number, Re, that depend on the permeability of the horizontal surfaces for fluid having $\mathrm{Pr} = 0.1$, and shown graphically in terms of streamlines, velocity vector and the isotherms of temperature at the steady-state situation. Numerical solutions are also presented in terms of local Nusselt number as well as average Nusselt number at the vertical surface. Finally a time history of the flow as well as the temperature distribution is displayed.

2. Mathematical formalisms

Consider the unsteady 2D flow of a viscous incompressible fluid in an open-ended cavity kept at temperature, T_C, which is same as that of the ambient fluid. The vertical wall opposite to the open end is maintained at a uniform temperature T_H. The horizontal surfaces of the cavity are assumed to be permeable with temperature same as that of the ambient fluid. The transpiration velocity of the fluid at the upper and lower surfaces is considered to be uniform. The effects of viscous dissipation and radiation are neglected. The variation of density with temperature follows the Boussinesq approximation. The geometry and the flow configuration are shown in Figure 1.

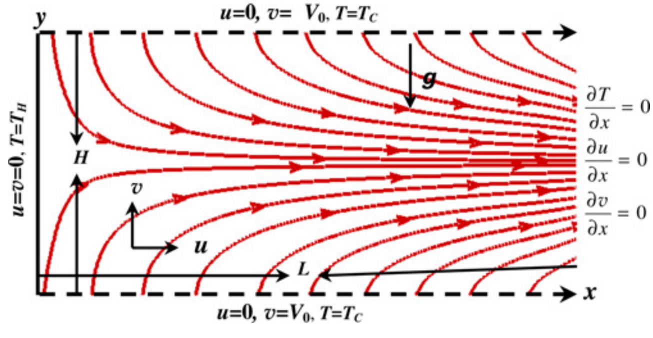

Figure 1.
The flow configuration and the coordinate system

Under the above assumptions the equations governing the 2D flow of a viscous incompressible fluid are as follows:

$$\frac{\partial u}{\partial x}+\frac{\partial v}{\partial y}=0 \tag{1}$$

$$\frac{\partial u}{\partial t}+u\frac{\partial u}{\partial x}+v\frac{\partial u}{\partial y}=-\frac{1}{\rho}\frac{\partial p}{\partial x}+\nu\left(\frac{\partial^2 u}{\partial x^2}+\frac{\partial^2 u}{\partial y^2}\right) \tag{2}$$

$$\frac{\partial v}{\partial t}+u\frac{\partial v}{\partial x}+v\frac{\partial v}{\partial y}=-\frac{1}{\rho}\frac{\partial p}{\partial y}+\nu\left(\frac{\partial^2 v}{\partial x^2}+\frac{\partial^2 v}{\partial y^2}\right)+g\beta_T(T-T_C) \tag{3}$$

$$\frac{\partial T}{\partial t}+u\frac{\partial T}{\partial x}+v\frac{\partial T}{\partial y}=\alpha\left(\frac{\partial^2 T}{\partial x^2}+\frac{\partial^2 T}{\partial y^2}\right) \tag{4}$$

where u and v are the x and y components of the velocity field, respectively, K is the permeability of the porous medium, g is the acceleration due to gravity, β_T is the volumetric expansion coefficients for temperature and α is the thermal diffusivity. Further, T is the temperature of the fluid flow and the time is t. In this study we have neglected stratification, viscous dissipation and other additional effects such as local thermal non-equilibrium.

Boundary conditions to be satisfied by the above equations are:

$$u(x,y)=0,\quad v(x,y)=0,\quad T(x,y)=0\quad \text{for } \forall t\leq 0$$

otherwise,

$$\begin{gathered}u(0,y)=0,\quad v(0,y)=0,\quad T(0,y)=T_H\\ u(x,0)=u(x,H)=0,\quad v(x,0)=V_0,\quad v(x,H)=-V_0,\quad T(x,H)=T_C\\ \frac{\partial u}{\partial x}=0,\quad \frac{\partial v}{\partial x}=0,\quad \frac{\partial T}{\partial x}=0\quad \text{at } x=L\end{gathered} \tag{5}$$

Based on these reference quantities, the following dimensionless variables are constructed:

$$\begin{gathered}X=\frac{x}{H},\quad Y=\frac{y}{H},\quad \tau=\frac{V_0}{H}t\\ U=\frac{u}{V_0},\quad V=\frac{v}{V_0},\quad G=\frac{T-T_C}{T_H-T_C}\end{gathered} \tag{6}$$

By introducing the above dimensionless dependent and independent variables in the governing equations the following equations are obtained:

$$\frac{\partial \Omega}{\partial \tau}+\frac{\partial (U\Omega)}{\partial X}+\frac{\partial (V\Omega)}{\partial Y}=\frac{1}{\mathrm{Re}}\left(\frac{\partial^2}{\partial X^2}+\frac{\partial^2}{\partial Y^2}\right)\Omega-\frac{Ra}{\mathrm{PrRe}}\frac{\partial G}{\partial X} \tag{7}$$

$$\frac{\partial G}{\partial \tau}+\frac{\partial (UG)}{\partial X}+\frac{\partial (VG)}{\partial Y}=\frac{1}{\mathrm{PrRe}}\left(\frac{\partial^2}{\partial X^2}+\frac{\partial^2}{\partial Y^2}\right)G \tag{8}$$

where,

$$\Omega = -\left(\frac{\partial^2}{\partial X^2} + \frac{\partial^2}{\partial Y^2}\right)\psi \tag{9}$$

is the vorticity directed in the *z*-direction, and ψ is the stream function defined by:

$$U = \frac{\partial \psi}{\partial Y}, \quad V = -\frac{\partial \psi}{\partial X} \tag{10}$$

In the above equations:

$$Ra = \frac{g\beta_T(T_1 - T_0)H^3}{\alpha\nu}, \quad \mathrm{Re} = \frac{V_0 H}{\nu}, \quad \mathrm{Pr} = \frac{\nu}{\alpha} \tag{11}$$

are, respectively, the Rayleigh number due to thermal diffusion, the Reynolds number due to permeability and the Prandtl number.

The boundary conditions are as follows:

$$\psi(X, Y) = 0, \quad \Omega(X, Y) = 0, \quad G(X, Y) = 0 \quad \text{at } \tau = 0$$

otherwise,

$$\begin{aligned}
&\psi = 0, \quad \Omega = \frac{\partial V}{\partial X}, \quad G = 1 \quad \text{at } X = 0 \\
&\frac{\partial \psi}{\partial X} = 0, \quad \frac{\partial \Omega}{\partial X} = 0, \quad \frac{\partial G}{\partial X} = 0 \quad \text{at } X = A \\
&\psi = 0, \quad \Omega = -\frac{\partial U}{\partial Y}, \quad G = 0 \quad \text{at } Y = 0 \quad \text{and} \quad 1 \\
&\frac{\partial \psi}{\partial X} = S \quad \text{at } Y = 0 \quad \text{and} \quad \frac{\partial \psi}{\partial X} = -S \quad \text{at } Y = 1
\end{aligned} \tag{12}$$

In equation (12), S is 1 and –1 while fluid is being sucked or blown through the horizontal permeable surfaces and $A = L/H$ measures the dimensionless length of the cavity.

Once we know the numerical values of the temperature θ we may obtain the rate of heat flux from each of the walls since the non-dimensional heat flux from any surface is given by $-(\partial T/\partial n)$, where n is the direction normal to the wall. For example, the non-dimensional heat transfer rate in terms of local Nusselt number, Nu, from the left vertical heated surface is given by:

$$Nu = -\left(\frac{\partial G}{\partial X}\right)_{X=0} \tag{13}$$

The corresponding value of the average Nusselt number, denoted by Nu_a, may be calculated from the following relation:

$$Nu_a = -\int_0^1 \frac{\partial G}{\partial X}\, dY \quad \text{at } X = 0 \tag{14}$$

3. Method of solution

An upwind finite-difference method, together with a successive over-relaxation (SOR) iteration technique, has been employed to integrate model equations (7) and (10) subject to the boundary conditions given in equation (12). To do this, the first and second derivatives were approximated by central differences and were used in the vorticity, energy and Poisson equations. To preserve the conservative property, the finite-difference forms of the vorticity and energy equations were written in conservative form for the convective terms. Values of the stream function at all grid points were obtained with equation (9) via an SOR method. The values for the relaxation parameters ω has been considered as:

$$\omega = \left(8 - 4\sqrt{4 - a^2}\right)/a^2 \quad \text{where } a = \cos\left(\frac{\pi}{m}\right) + \cos\left(\frac{\pi}{n}\right) \tag{15}$$

In the above relation m and n represent the number of subintervals along X- and Y-direction, respectively. The velocities at all grid points were determined with the dimensionless form of equation (10) using updated values of the stream function. Variations by less than 10^{-5} over all grid points for the stream function were adopted as the convergence criterion.

A grid dependence study has been carried out, as done by Hossain and Wilson (2004), Hossain and Rees (2003, 2005), and Hossain and Gorla (2006) for a thermally driven cavity flow, for different values of the physical parameters, with meshes of 41×41, 51×51 and 61×61 points. It has been found that there are very small differences in the maximum or minimum values of the stream function between above sets of meshes. Here we have demonstrated the numerical values of $|\psi|_{max}$ in Table I at mesh-points 175×51, 201×51, 225×51 and 201×61 while Re $= 102$, $Ra = 106$ and $S = 1$ at steady-state situation, from which one can see very small difference between the values at different mesh-points. Hence we have chosen to use 201×61 mesh-points throughout the present computations with a time step of 5×10^{-6} until the dimensionless time reaches $\tau = 5.0$. This value for τ was found to be sufficient to reach to the steady-state situation for the fluid of Pr $= 0.1$.

In Figure 2 we demonstrate the values of the Nusselt number, Nu_a, along the heated surface of the open-ended rectangular cavity, against Y. In this figure the graphs are for Ra equal to 10^6, while Re $= 100$ and $S = -1$ for mesh-points 175×51, 201×51, 225×51 and 201×61. As before we may conclude that choice in mesh-points, either 225×51 or 201×61, is sufficient for the overall numerical simulations. Finally, it should be mentioned that, using the present method we have revisited the work of Angirasa *et al.* (2002) for the case where three solid surfaces were considered to be heated. And some results are shown in Figure 3, which are found to agree well with those obtained by these authors.

Most of the results obtained from the present investigation will be discussed in the following section considering the fluid for which Pr $= 0.1$.

Table I. Numerical values of $|\psi|_{max}$ at different $m \times n$ while Re $= 10^2$, $Ra = 10^6$ and $S = 1$

$m \times n$	175×51	201×51	225×51	201×61
$\lvert\psi\rvert_{max}$	4.185	4.183	4.182	4.183

4. Results and discussion

Investigation of unsteady, laminar natural convection flow of a viscous incompressible fluid in an open-ended rectangular cavity having permeable horizontal surfaces has been made. For numerical simulation of the dimensionless equations that govern the flow, the finite-difference approach along with the SOR iteration technique has been employed, considering the fact that both the horizontal surfaces are colder than the left vertical one and having the temperature of the ambient fluid.

The non-dimensional controlling parameters are the Rayleigh number, *Ra*, the Prandtl number, Pr and the Reynolds number, Re (that depends on the permeability of the horizontal surfaces). Throughout the present investigation the length, *A*, of the cavity has been chosen to be 4 and the fluid of Pr equal to 0.1.

Taking into consideration impermeable horizontal adiabatic surfaces, Chan and Tien (1982) investigated a 2D open cavity with only the vertical side heated. They used a primitive variable formulation, and the computational domain included the outer region. In an interesting way, they (Chan and Tien, 1985) also have explored the possibility of obtaining a set of boundary conditions for primitive variables at the cavity window for computing within the domain of the cavity. The results indicated that natural convection inside the cavities was not much influenced by the far field. Very close to the present work, Angirasa *et al.* (2002) presented a numerical study of a square open cavity with the one vertical side heated, solving for vorticity transport and stream function. In this investigation the computations were performed without an outer region by specifying an appropriate set of boundary conditions at the window.

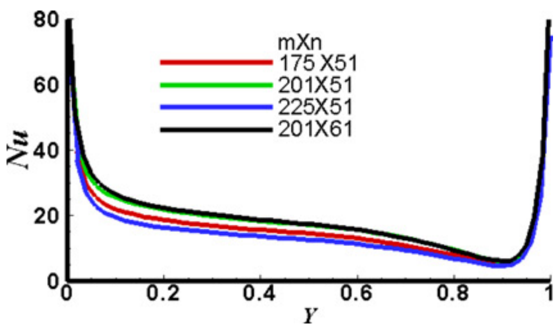

Figure 2. Numerical values of Nusselt number, *Nu*, at different mesh-points while $\mathrm{Re} = 10^2$, $Ra = 10^6$ and $S = 1$

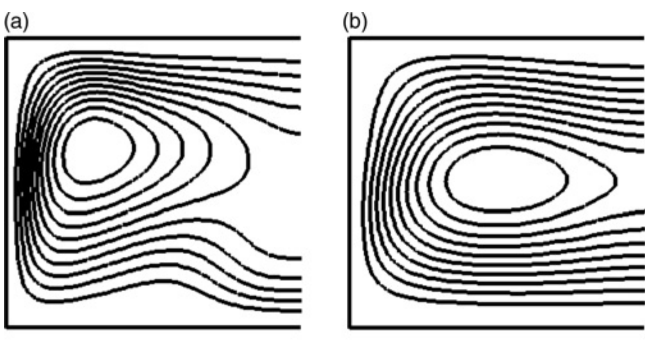

Notes: (a) $\tau = 5$ and (b) $\tau = 5$
Source: Angirasa *et al*. (2002)

Figure 3. Streamlines at $\tau = 4$, $\mathrm{Pr} = 0.7$, $Ra = 10^5$ for the case when the three solid surface are heated

The solutions of the temperature and vorticity equations were obtained using the alternating direction implicit (ADI) implicit scheme and the SOR method was employed to obtain solution for stream function. They also studied transient solutions of tie flow and heat transfer to check the validity of the boundary conditions as the solution evolves. It is worth mentioning that using the present method we have revisited the work of Angirasa *et al.* (2002), for the case where three solid surfaces were considered to be heated. And some results are shown in Figure 3, which are found to agree well with those obtained by these authors.

Transient velocity field, streamlines and isotherms

We, now, first show the time history through streamlines and velocity vectors taking $Ra = 10^6$ and $\mathrm{Re} = 10^2$ while fluid is being withdrawn through the permeable surface in Figure 4. It can be seen from this figure that there develops vortex motion with low intensity along the heated surface. The intensity and the size of the vorticity increase with time and finally reach the steady state. In the present investigation it is seen that the steady-state situation is reached at $\tau = 4$.

Effect of Rayleigh number, Ra, *on velocity field, streamlines and isotherms and Nusselt number*

Now we show the effect of different Rayleigh number, *Ra*, namely, 0.0, 10^4, 10^5 and 10^6 on the velocity vectors and the streamlines, as well as on the isotherms for withdrawal and blowing of fluid through the permeable surface through Figures 5 and 6, respectively. From Figure 5, in case of withdrawal of fluid, an increase in the value of *Ra* destroys the symmetry in the flow within the cavity. At a higher value of the Rayleigh number there develops vortex motion near the heated surface, which is expected, since, in this case, domination of buoyancy force prevails ($Ra > \mathrm{Re}$). From the corresponding isotherms we see that the buoyancy force also enhances the temperature of the fluid in the region near the upper surface of the cavity.

In Figure 6, displayed are the streamlines and the velocity vectors showing the effect of increasing value of the Rayleigh number, *Ra*, at steady state when fluid is being blown through the permeable surfaces. Corresponding isotherms are also shown in the right column of this figure. From this figure we also see that, similar to the case of withdrawal of fluid, an increase in the value of the Rayleigh number distorts the symmetry of the flow and enhances the flow velocity. At higher value of *Ra*, there develops a vortex motion in the upper half regime and also there is elongation of the vortex. Further we notice that the intensity of the flow near the outlet of the cavity also increases owing to an increase in the

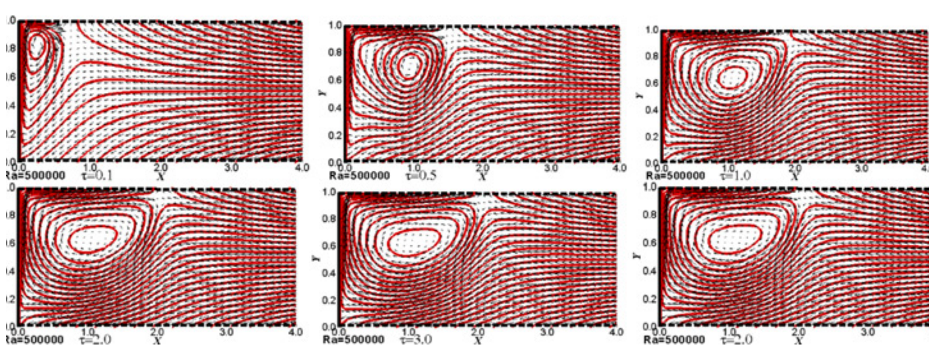

Figure 4.
Time history of velocity vectors and streamlines while fluid is being sucked through the permeable surface ($S = 1$) at $Ra = 10^6$ and $\mathrm{Re} = 10^2$

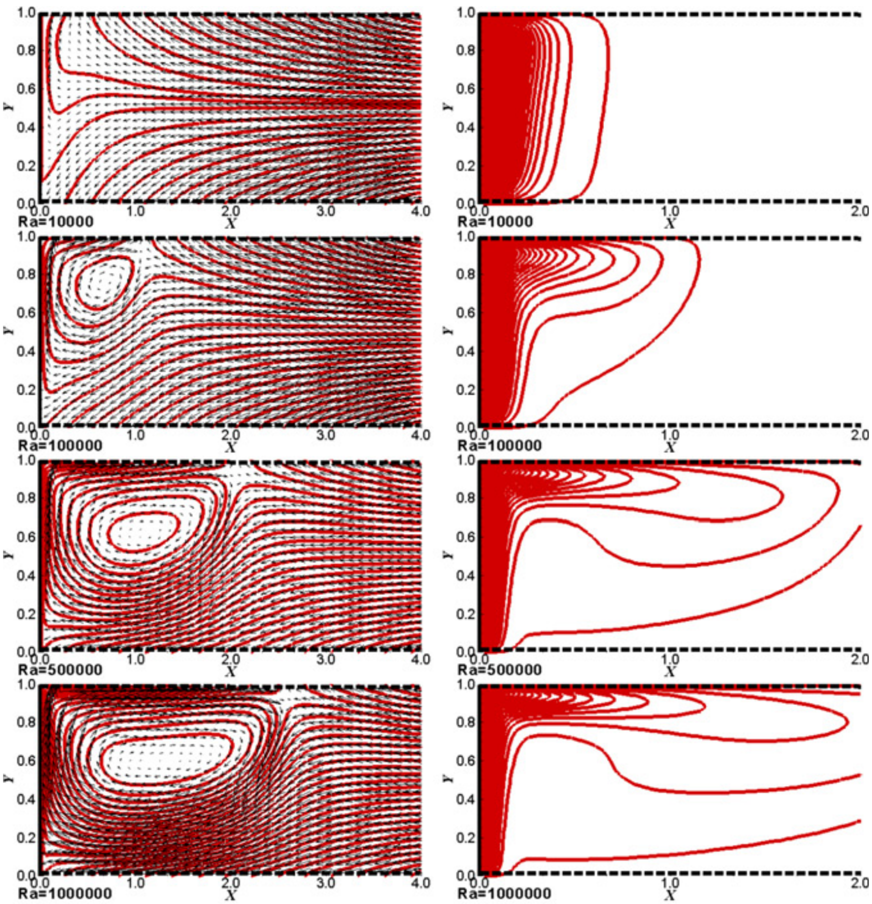

Notes: (Left) velocity vectors and streamlines and (right) isotherms for $Ra = 10^4, 10^5$, 5×10^5 and 10^6 while $\mathrm{Re} = 10^2$ at $S = 1$ (withdrawal of fluid through the horizontal surfaces)

Figure 5.

value of *Ra*. An increase in the buoyancy force causes an increase in the temperature distribution from the heated surface (can be seen from the isotherms) and thus enhances the velocity of the fluid particles. It can further be seen that there is an increase in both momentum and thermal boundary layers due to an increase in the value of *Ra*. It is obvious, since, when $Ra \gg \mathrm{Re}$, the buoyancy force will dominate the mass flux through the surface. Finally, in the present physical condition, the flow remains stable until *Ra* reaches a value of 1.75×10^6. Further numerical calculations show that this critical value of *Ra* increases due to an increase in the value of the Reynolds number, Re (that depends on the transpiration velocity) or at reduced cavity height.

Now we show the effect of increasing value of the Rayleigh number on the local Nusselt number (or the rate of heat transfer) at the heated wall for the case when fluid is being sucked as well as blown through the permeable surface in Figure 7 taking $\mathrm{Re} = 10^2$. From this figure, it can be seen that the local heat transfer increases with an

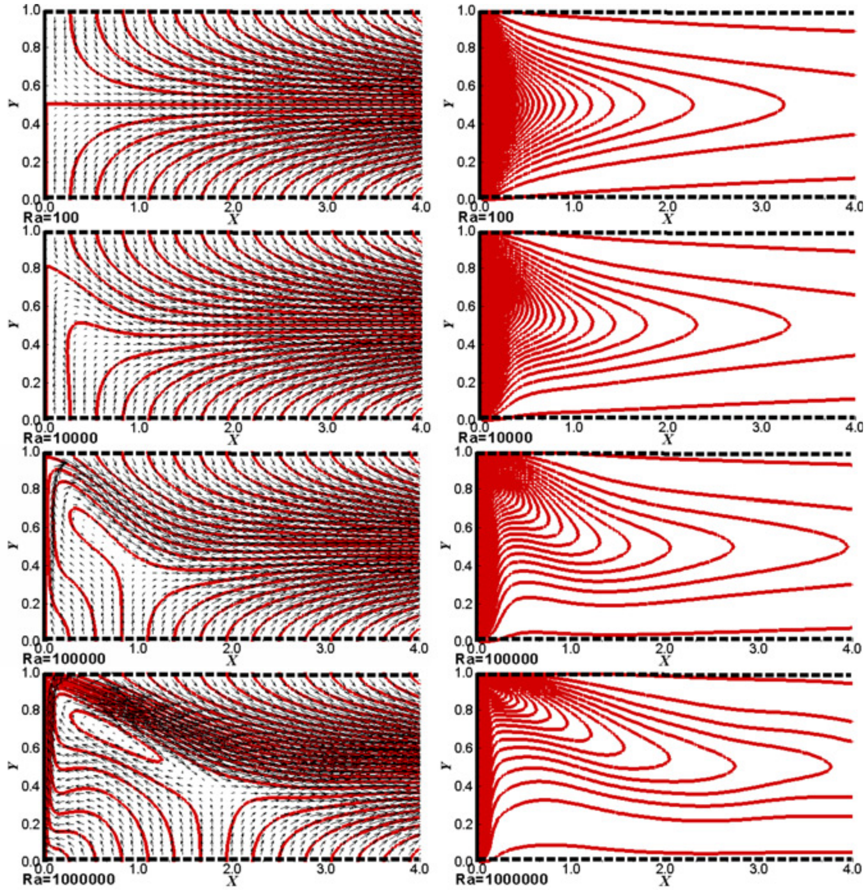

Figure 6.

Notes: (Right) velocity vectors and streamlines and (left) isotherms for $Ra = 10^2, 10^4, 10^5$ and 10^6 while $\mathrm{Re} = 10^2$ at $S = 1$ (blowing of fluid through the horizontal surfaces)

increase in the value of *Ra*. We can further observe that, in the region near the bottom surface, the heat transfer from the left vertical surface decreases and increases in the region near the upper surface. Comparison between the results for $S = 1$ (withdrawal of fluid) and –1 (blowing of fluid) shows that due to blowing of fluid through the permeable surface the rate of heat transfer is higher than the situation where fluid is being withdrawn through the permeable surface. This difference is higher in case of larger value of *Ra*.

In Figure 8, we have depicted the numerical values of the average Nusselt number against τ for different values of the Rayleigh number, *Ra*. From this figure we can see that, for both the cases when fluid is being sucked or blown through the surfaces, the average heat transfer decreases at $Ra = 10^4$ and 10^5 and increases while $Ra = 10^6$ when $\tau < 0.2$, which reaches the steady-state value. As in the case of local Nusselt number, the value of the average Nusselt number is higher when fluid is being blown through the permeable surfaces (i.e. when $S = -1$).

Effect of Reynolds number, Re, on velocity field, streamlines and isotherms and Nusselt number

Now we show the effect of surface mass flux that will increase the value of the Reynolds number Re on the velocity and streamlines, at $Ra = 10^6$, in the situation where fluid is being sucked as well as blown through in Figure 9. The streamlines and the velocity vectors presented in left column are those with suction of fluid. From this figure, one can see that the cell that developed in the region at the left top corner of the cavity is disappearing with the creasing value of Re, which is expected, since suction phenomena will take the heated fluid particles which ultimately dominate the effect of buoyancy force along the heated surface. Finally, at larger value of Re, the flow variables become symmetric about the central line in the horizontal axis and there is no instability. From the right column of this figure one can notice a similar flow phenomenon when the fluid is blown through the permeable surfaces.

Finally, Figure 10 depicts the average Nusselt number for $S = 1.0$ and -1 and $Ra = 10^6$ against τ for different values of Re that shows the effect of increasing surface mass flux. As Re increases, the value of the average Nusselt number increases for both cases when fluid is being sucked as well as injected. Comparison between the black broken curves with the solid dark grey curves shows that at larger value of Re, it is seen that the average Nusselt number is considerably higher when fluid is being sucked than that of blowing of fluid through the permeable surfaces.

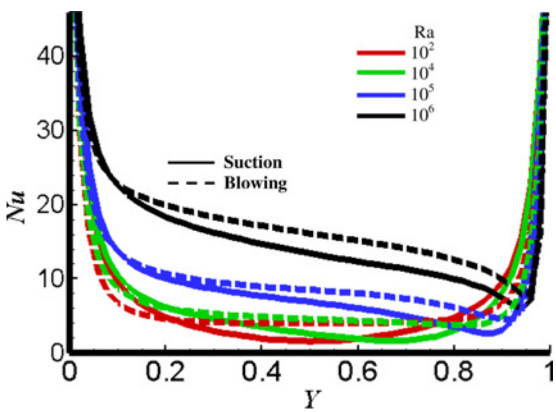

Figure 7. Numerical values of Nusselt number, Nu, against Y at the heated surface for different values of Ra when $S = 1$ and -1

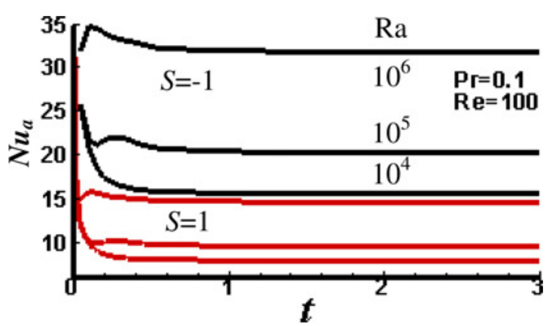

Figure 8. Numerical values of average Nusselt number, Nu_a, against Y at the heated surface for different values of Ra when $S = 1$ and -1

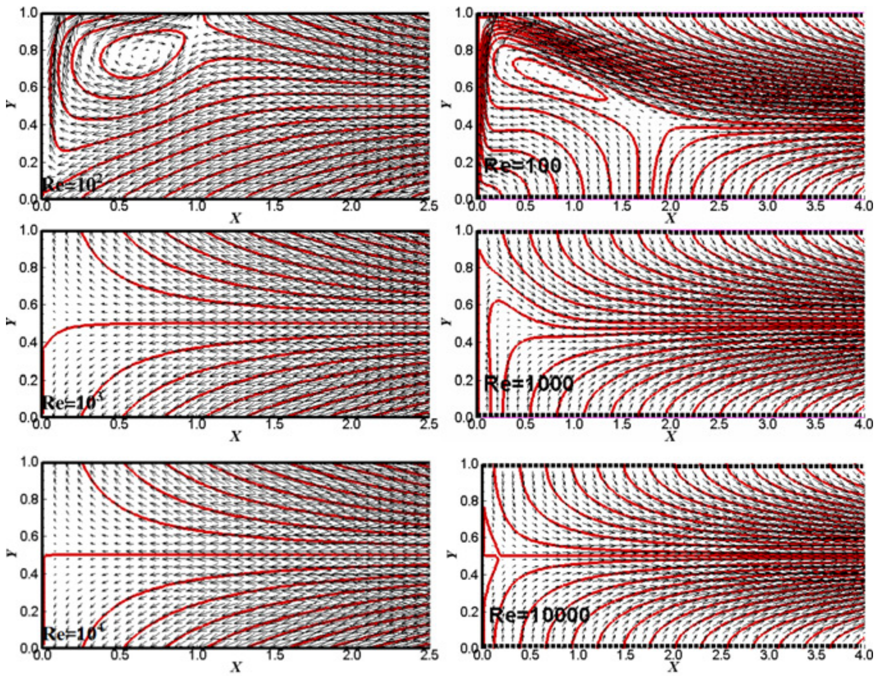

Figure 9.
Effect of Reynolds number ($Re = 10^2$, $Re = 10^3$, $Re = 10^4$) on the streamlines and velocity vectors

Notes: While $Ra = 10^6$: (left) $S = 1$ and (right) $S = -1$

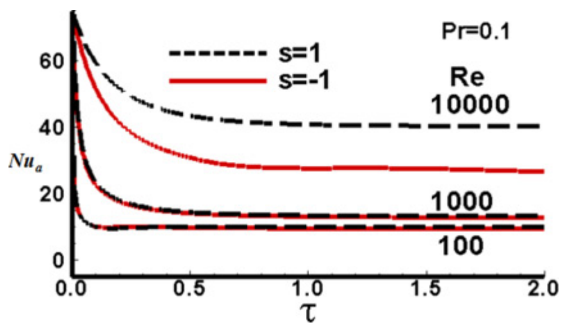

Figure 10.
Numerical values of average Nusselt number, Nu_a, against τ at different values of Re while $Ra = 10^6$ and $S = 1, -1$

Conclusions

In the present paper, investigation has been made on the unsteady natural convection flow of viscous incompressible fluid filled in an open-ended rectangular enclosure. Two permeable horizontal surfaces of the cavity are maintained at temperature same as that of the ambient fluid considering the fact that the temperature of vertical solid surface is higher than that of the horizontal surfaces. The governing equations for the flow are simulated numerically by employing an upwind finite-difference method together with an SOR technique. Results are obtained for values of the Rayleigh number, Ra, equal to 10^4, 10^5 and 10^6 whereas the Reynolds number, Re (that depends on the permeability of the horizontal surfaces), ranges from 10^2 to 10^4 and the Prandtl number, Pr, is equal to 0.1, which is appropriate for liquid metal and semi-conductor melt.

The following conclusions may be drawn from the present investigations:

- At higher value of the Rayleigh number there develops a vortex motion near the heated surface, for $Ra > \mathrm{Re}$. Buoyancy force also enhances the temperature of the fluid in the region near the upper surface of the cavity.
- Intensity of the flow near the outlet of the cavity increases owing to an increase in the value of Ra.
- Local rate of heat transfer from the heated surface increases owing to an increase in the value of Ra. In the region near the bottom surface, the heat transfer from the left vertical surface decreases, but that increases in the region near the upper surface. Due to blowing of fluid through the permeable surfaces, the rate of heat transfer is higher than the situation where fluid is being withdrawn. This difference was found to be higher in the case of larger value of Ra.
- Average Nusselt number is higher when fluid is being blown through the permeable surfaces (i.e. when $S = -1$).
- At larger value of Re, the flow variables become symmetric about the central line in the horizontal axis and there is no instability. Similar phenomenon occurs when the fluid is being blown through the permeable surfaces.

References

Angirasa, D., Pourquie, M.J.B.M. and Nieuwstadt, F.T.M. (1996), "Numerical study of transient and steady laminar buoyancy-driven flows and heat transfer in a squire open-cavity", *Numerical Heat Transfer, Part A*, Vol. 22, pp. 223-39.

Angirasa, D., Pourquie, M.J.B.M. and Nieuwstadt, F.T.M. (2002), "Numerical simulation of transient natural convection from an isothermal cavity open on a side", *Numerical Heat Transfer, Part A*, Vol. 28, pp. 755-68.

Bilgen, E. and Oztop, H. (2005), "Natural convection heat transfer in partially open inclined square cavities", *International Journal of Heat and Mass Transfer*, Vol. 48, pp. 1470-9.

Chan, Y.L. and Tien, C.L. (1982), "A numerical study of 2D natural convection in square open cavities", *Numerical Heat Transfer*, Vol. 8, pp. 65-80.

Chan, Y.L. and Tien, C.L. (1985), "A numerical study of 2D laminar natural convection in shallow open cavities", *International Journal of Heat and Mass Transfer*, Vol. 28, pp. 603-12.

Chen, K.S., Humphery, J.A.C. and Sherman, F.S. (1985), "Experimental investigation of thermally driven flow in open cavities of rectangular cross-section", *Philosophical Transactions of the Royal Society of London, Series A*, Vol. 316, pp. 57-84.

Doria, M.L. (1974), "A numerical model for the prediction of 2D unsteady flows of multi-component gases with strong Buoyancy effects and recirculation", Notre Dame Report No. TR-37191-74-4.

Hossain, M.A. and Gorla, R.S.R. (2006), "Effect of viscous dissipation on mixed convection flow of water near its density maximum in a rectangular enclosure with isothermal wall", *International Journal of Numerical Methods for Heat & Fluid Flow*, Vol. 16, pp. 5-17.

Hossain, M.A. and Rees, D.A.S. (2003), "Natural convection flow of viscous incompressible fluid in a rectangular porous cavity heated from below with cold side walls", *Heat and Mass Transfer*, Vol. 39, pp. 657-63.

Hossain, M.A. and Rees, D.A.S. (2005), "Natural convection flow of water near its density maximum in a rectangular enclosure having isothermal walls with heat generation", *Heat and Mass Transfer*, Vol. 41, pp. 367-74.

Hossain, M.A. and Wilson, M. (2004), "Natural convection flow in a fluid-saturated porous medium enclosed by non-isothermal walls with heat generation", *International Journal of Thermal Sciences*, Vol. 41, pp. 447-54.

Jacobs, H.R. and Mason, W.E. (1976), "Natural convection in open rectangular cavities with adiabatic sidewalls", *Proceedings of the 1976 Heat Transfer and Fluid Mechanics Institute*, *Stanford University Press*, *Stanford, CA*, pp. 33-46.

Jacobs, H.R., Mason, W.E. and Hikida, W.T. (1974), "Natural convection in open rectangular cavities", *Proceedings of Fifth International Heat Transfer Conference, Tokyo*, Vol. 3, pp. 90-4.

Mohamad, A.A., El-Ganaoui, M. and Bennacer, R. (2009), "Lattice Boltzmann simulation of natural convection in an open ended cavity", *International Journal of Thermal Sciences*, Vol. 48, pp. 1870-5.

Müftüŏglu, A. and Bilgen, E. (2008), "Natural convection in an open square cavity with discrete heaters at their optimized positions", *International Journal of Thermal Sciences*, Vol. 47, pp. 369-77.

Penot, F. (1982), "Numerical calculation of 2D natural convection in isothermal open cavities", *Numerical Heat Transfer*, Vol. 5, pp. 421-37.

Serans, V. and Kyriakides, I. (1982), "Natural convection in an open cavity", *Proceedings of the Seventh International Heat Transfer Conference, Munchen*, Vol. 2, pp. 275-86.

Vafai, K. and Ettefagh, J. (1990a), "The effects of sharp corners on buoyancy-driven flows with particular emphasis on outer boundaries", *International Journal of Heat and Mass Transfer*, Vol. 33, pp. 2311-28.

Vafai, K. and Ettefagh, J. (1990b), "Thermal and fluid flow instabilities in buoyancy-driven flows in open-ended cavities", *International Journal of Heat and Mass Transfer*, Vol. 33, pp. 2329-44.

Corresponding author
Rama Subba Reddy Gorla can be contacted at: r.gorla@csuohio.edu